



## Leukocyte-specific siRNA delivery revealing IRF8 as a potential anti-inflammatory target



Nuphar Veiga<sup>a,b,c,d,e</sup>, Meir Goldsmith<sup>a,b,c,d,e</sup>, Yael Diesendruck<sup>b</sup>, Srinivas Ramishetti<sup>a,b,c,d,e</sup>, Daniel Rosenblum<sup>a,b,c,d,e</sup>, Eran Elinav<sup>f</sup>, Mark A. Behlke<sup>g</sup>, Itai Benhar<sup>b</sup>, Dan Peer<sup>a,b,c,d,e,\*</sup>

<sup>a</sup> Laboratory of Precision NanoMedicine, Tel Aviv, 69978, Israel

<sup>b</sup> School of Molecular Cell Biology and Biotechnology, George S. Wise Faculty of Life Sciences, Tel Aviv, 69978, Israel

<sup>c</sup> Department of Materials Sciences and Engineering, Iby and Aladar Fleischman Faculty of Engineering, Tel Aviv, 69978, Israel

<sup>d</sup> Center for Nanoscience and Nanotechnology, Tel Aviv, 69978, Israel

<sup>e</sup> Cancer Biology Research Center, Tel Aviv University, Tel Aviv, 69978, Israel

<sup>f</sup> Immunology Department, Weizmann Institute of Science, Rehovot, Israel

<sup>g</sup> Integrated DNA Technologies, Inc., Coralville, IA, 52241, USA

### ARTICLE INFO

#### Keywords:

IBD  
Nanoparticle  
LNP  
IRF8  
Immunomodulation  
RNAi

### ABSTRACT

Interferon regulatory factor 8 (IRF8) protein plays a critical role in the differentiation, polarization, and activation of mononuclear phagocytic cells. In light of previous studies, we explored the therapeutic potential of IRF8 inhibition as immunomodulatory therapy for inflammatory bowel disease (IBD). To this end, we utilized siRNA-loaded lipid-based nanoparticles (siLNPs) and demonstrated a ~90% reduction of IRF8 mRNA levels *in vitro* (PV < 0.0001), alongside a notable reduction in IRF8 protein. Moreover, silencing IRF8 *ex vivo* in splenocytes lead to a profound downregulation of IRF8 protein, followed by an immunomodulatory effect, as represented by a decrease in the secretion of TNF $\alpha$ , IL6 and IL12/IL23 (IL12p40) proinflammatory cytokines (PV = 0.0045, 0.0330, < 0.0001, respectively). In order to silence IRF8 *in vivo*, selectively in inflammatory leukocytes, we used siLNPs that were coated with anti-Ly6C antibodies *via* our recently published ASSET targeting approach. Through this strategy, we have demonstrated a selective binding of the targeted-LNPs (T-LNPs) to Ly6C + inflammatory leukocytes. Finally, an immunomodulatory effect was demonstrated *in vivo* in an IBD mouse model with a profound decrease of TNF $\alpha$ , IL6, IL12/IL23, and IL1 $\beta$  pro-inflammatory cytokines (n = 5, PV < 0.0001, < 0.0001, < 0.0001, 0.02, respectively) and an improvement of colon-morphology as assessed by colon-length measurements and colonoscopy (PV < 0.0001). Overall, using antibody-targeted siLNPs, we showed a notable reduction of IRF8 mRNA and protein and demonstrated a targeted immunomodulation therapeutic effect *ex vivo* and *in vivo*, in the DSS colitis model. We claim that a selective silencing of IRF8 in inflammatory leukocytes (such as Ly6C+) may serve as a therapeutic approach for treating inflammatory disorders.

### 1. Introduction

Inflammatory Bowel Disease (IBD), such as Crohn's Disease and Ulcerative Colitis, is a group of inflammatory disorders that affect the gastrointestinal tract. The global increase in IBD incidence is closely related to environmental and lifestyle changes. However, with a multifactorial nature and a complex interaction between microbiota, genetics and environmental factors, the etiology of IBD remains unclear. [1,2] During the past few decades, progress in the development of novel immunomodulatory remedies significantly improved the patient's quality of life. Such treatment modalities include blocking of intestinal

leukocytes infiltration by anti-adhesion agents (e.g. Vedolizumab, Etrolizumab), inhibiting pro-inflammatory mediators, such as TNF $\alpha$  (e.g. Infliximab, Adalimumab), and IL12/IL23 (Ustekinumab). Further treatments of IBD include JAK/STAT1 inhibition (Tofacitinib), intestinal trafficking blocking (Ozanimod) and microbiome manipulation. However, several aspects are diminishing the effectiveness of clinically available treatments, including low response rate, resistance pathways, generation of antibodies against the mAb ('ADA' phenomena), opportunistic infections, and diverse adverse effects [3].

Healthy intestinal homeostasis is actively balanced by immune cells [4]. When this balance is disrupted, activated immune cells accumulate

\* Corresponding author at: Laboratory of Precision NanoMedicine, Tel Aviv, 69978, Israel.

E-mail address: [peer@tauex.tau.ac.il](mailto:peer@tauex.tau.ac.il) (D. Peer).

<https://doi.org/10.1016/j.jconrel.2019.10.001>

Received 6 September 2019; Received in revised form 3 October 2019; Accepted 4 October 2019

Available online 18 October 2019

0168-3659/ © 2019 Elsevier B.V. All rights reserved.

in the affected area and mediate a prominent intestinal inflammation *via* both humoral and cellular immune response. The numbers and subsets diversity of intestinal leukocytes is massively altered in IBD patients. For instance, CD14<sup>+</sup> leukocytes accumulate in the intestine of IBD patients and are responsible for the secretion of pro-inflammatory mediators. [5,6] In the murine dextran sodium sulfate (DSS) colitis model, which is widely used to study gastrointestinal disorders, similar phenomenon is observed by Ly6C<sup>+</sup> population of monocytes, macrophages, and dendritic cells. [7–9] Ly6C<sup>+</sup> leukocytes are recruited to the site of inflammation and are responsible for the production of several proinflammatory cytokines, such as TNF $\alpha$  and IL6. [7,9] Thus, inhibiting the pro-inflammatory characteristics of Ly6C<sup>+</sup> leukocytes have a potential as an anti-inflammatory therapeutic approach for modulating IBD and other inflammatory disorders. [10–12]

The transcription factor Interferon Regulatory Factor 8 (IRF8) is involved in various immune-related pathways such as hematopoiesis, polarization, and activation. IRF8 plays a critical role in the differentiation, maturation, and activation of mononuclear phagocytic cells, including monocytes, macrophages and various subtypes of dendritic cells [13,14]. Furthermore, genetic variations in the *IRF8* gene were shown to correlate with increased susceptibility to several inflammatory disorders, such as multiple sclerosis, rheumatoid arthritis and IBD. [15] It was previously demonstrated that IRF8 is involved in the activation of Ly6C<sup>+</sup> leukocytes and mediate their proinflammatory responses as well as Th1 and Th17 polarization in mice. [16–20] Considering previous studies, we hypothesized that the inhibition of IRF8 can potentially serve as an immunomodulatory pathway in various inflammatory disorders, such as colitis and multiple sclerosis. However, since IRF8 is expressed by multiple cell lineages and play a distinct role in each cell type in various developmental stages, designing a clinically relevant approach requires a careful selective manipulation of IRF8 [13]. Dual targeting, where IRF8 is silenced only in the relevant leukocytes could serve such a purpose.

Nucleic acid loaded lipid nanoparticles (LNPs), which target subsets of inflammatory leukocytes, have emerged as a promising immunomodulatory approach. [10,11,21,22] Loaded with either siRNA or mRNA, LNPs demonstrate an innovative, safe and robust strategy to manipulate gene expression *in vivo*. Moreover, RNA loaded LNPs have exhibited an effective therapeutic potential in various diseases, including cancer and inflammation. Previously, we designed a modular targeting platform named Anchored Secondary scFv Enabling Targeting (ASSET). ASSET technology provides a non-covalent binding of rat IgG mAbs to the LNPs surface and thus facilitate the construction of a theoretically unlimited repertoire of targeted LNPs (T-LNPs). Utilizing the ASSET system to selectively transfect Ly6C<sup>+</sup> cells with RNA molecules, we exhibited an efficient manipulation of cytokines' secretion as an effective therapeutic approach for IBD. [10,11] Upon the first-ever FDA approval of Pattisiran (Onpattro™) in August 2018 for hereditary TTR amyloidosis, RNA loaded LNPs appear as a promising and flexible therapeutic strategy, which can potentially serve as a treatment for diverse pathologies. Moreover, a flexible T-LNPs technology can potentially serve as a research tool, aiming to identify new targets for therapy in varied diseases. Therefore, utilizing antibodies-targeted siRNA loaded LNPs for the regulation of IRF8 levels in Ly6C<sup>+</sup> cells could serve as a therapeutically relevant pathway for controlling inflammatory disorders, as IBD.

Here we utilized targeted LNPs to explore the role of IRF8 as a novel potential target for anti-inflammatory therapy. We established a discerning method for inhibiting IRF8 expression, using siRNA, in inflammatory Ly6C<sup>+</sup> leukocytes *ex vivo* and *in vivo*, thus balancing the secretion of pro-inflammatory cytokines. Furthermore, using targeted delivery of IRF8 siRNA molecules to inflammatory Ly6C<sup>+</sup> leukocytes *in vivo*, we were able to demonstrate a significant anti-inflammatory effect in the DSS colitis mouse model. IRF8 silencing in Ly6C<sup>+</sup> subsets resulted in a decrease in the colon's pro-inflammatory cytokines levels, an improvement of colon's morphology and reduction in colon's

inflammation. Altogether, we believe that selective silencing of IRF8 in inflammatory Ly6C<sup>+</sup> has potential as a novel therapeutic modality for treating IBD and perhaps additional inflammatory disorders.

## 2. Materials and methods

### 2.1. Monoclonal antibodies used in these studies

$\alpha$ Ly6c (clone Monts1, BioXcell)  
 Rat IgG2a isotype control (clone 2A3, BioXcell)  
 $\alpha$ Ly6c (clone HK1.4, Biolegend)  
 $\alpha$ IRF8 (clone V3GYWCH, eBioscience)  
 Mouse IgG1 kappa isotype control (clone P3.6.2.8.1, eBioscience)  
 $\alpha$ CD45 (clone 30-F11, Biolegend)  
 $\alpha$ CD19 (clone 6D5, Biolegend)  
 $\alpha$ CD11b (clone M1/70, Biolegend)  
 $\alpha$ CD4 (clone GK1.5, Biolegend)  
 $\alpha$ CD8 (clone 53.6.7, Biolegend)  
 $\alpha$ CD3 (clone 145-2C11, Biolegend)  
 $\alpha$ IRF8 polyclonal (ThermoFisher)  
 $\alpha$ Rabbit conjugated to HRP (Jackson ImmunoResearch)  
 $\alpha$ Rat conjugated to HRP (Jackson ImmunoResearch)

### 2.2. Cell lines

RAW 264.7 cells (ATCC, TIB-71). All cells were routinely checked every two months for Mycoplasma contamination using EZ-PCR Mycoplasma Test Kit (Biological Industries) according to the manufacture's protocol.

### 2.3. siRNAs

Chemically modified Dicer-substrate siRNAs against IRF8, negative control siRNA NC5 and NC5-Cy5 (siCy5) were synthesized at IDT (Coralville, Iowa, USA) using standard phosphoramidite chemistry and the following sequences.

IRF8-3 siRNA : 5' GUCUGUGACUAAGAGAAUUCGGAa 3', 5' UUUCGGAAUUCUCUUAGUCACAGACUC 3'

IRF8-9 siRNA : 5' GCCGCAACCUGUGAUUAAAGCAUc 3', 5' GAAUGCUUUAUUCACAGGUUGCGGCCA 3', where uppercase bases are RNA, uppercase underlined are 2'-O-methyl RNA, and lowercase are DNA.

### 2.4. Lipids

DSPC, Cholesterol, DMG-PEG 2000 and DSPE-PEG 2000 were purchased from Avanti Polar Lipids. Dlin-MC3-DMA (MC3) was synthesized according to a previously described method [11].

### 2.5. Primers

GAPDH Fwd: 5' TTG TGG AAG GGC TCA TGA CC 3'; GAPDH Rev: 5' TCT GGG TGG CAG TGA TG 3'; IRF8 Fwd: 5' CTA CCT GCA CCA GAA TGA GTT 3'; IRF8 Rev: 5' TGA CAC CAA CCA GTT CAT CC 3'; HPRT Fwd: 5' CCC CAA AAT GGT TAA GGT TGC 3'; HPRT Rev: 5' AAC AAA GTC TGG CCT GTA TCC 3'; STAT1 Fwd: 5' TTG ACA AAG ACC ACG CCT T 3'; STAT1 Rev: 5' GAC TTC AGA CAC AGA AAT CAA CTC 3'; Slc11a1 Fwd: 5' GCC TTC TAC CAG CAA ACC AA 3'; Slc11a1 Rev: 5' CCT TGA TAA ATA TCC ACT GAC A 3'; CCL5 Fwd: 5' GCT CCA ATC TTG CAG TCG T 3'; CCL5 Rev: 5' CCT CTA TCC TAG CTC ATC TCC A 3'; Cybb Fwd: 5' TGT TCC TGT ACC TTT GTG AGA G 3'; Cybb Rev: 5' CAC CTC CAT CTT GAA TCC CTT 3'; Spi1 Fwd: 5' TGA TCC CCA CCG AAG CA 3'; Sfp1 Rev: 5' CGT AAG TAA CCA AGT CAT CCG A 3'

## 2.6. Preparation of LNPs with entrapped siRNAs

LNPs were prepared according to previously described method (10). Briefly, one volume of lipid mixture (MC3, DSPC, Cholesterol, DMG-PEG, and DSPE-PEG-Ome at 50:10.5:38:1.4:0.1 mol ratio) in ethanol and three volumes of siRNA (1:16 w/w siRNA to lipid, 1 : 1 mol ratio of siIRF8-3 and siIRF8-9) in an acetate buffer were injected in to a microfluidic mixing device Nanoassemblr (Precision Nanosystems) at a combined flow rate of 2mlmin<sup>-1</sup> (0.5mlmin<sup>-1</sup> for ethanol and 1.5mlmin<sup>-1</sup> for aqueous buffer). The resultant mixture was dialyzed against phosphate buffered saline (PBS) (pH 7.4) for 16 h to remove ethanol. For Cy5-labelled particles, 15% Cy5-labelled NC5 siRNA were used for flow cytometry analysis and confocal microscopy.

## 2.7. Size distribution

LNP sizes in PBS were measured by dynamic light scattering using a Malvern nano-ZS Zetasizer (Malvern Instruments Ltd).

## 2.8. Transmission electron microscopy

A drop of aqueous solution containing siRNA loaded LNPs was placed on a carbon-coated copper grid and dried and analyzed using a JEOL 1200 EX transmission electron microscope.

## 2.9. ASSET LNP incorporation and TsiLNP assembly

ASSET was incorporated into the LNPs as previously described method (10), by an incubation of ASSET micelles with LNPs for 48 h at 4 °C (1:36, ASSET:siRNA weight ratio).

## 2.10. siRNA encapsulation efficiency

The efficiency of siRNA encapsulation was determined by Quant-iT RiboGreen RNA assay (Life Technology) as previously described [10]. Briefly, 2 µl of LNPs or dilutions of siRNA at known concentrations were diluted in a final volume of 100 µl of TE buffer (10 mM Tris–HCl, 20 mM EDTA) and 0.5% Triton X-100 (Sigma-Aldrich) in a 96-well fluorescent plate (Costar, Corning). The plate was incubated for 10 min at 40 °C to allow particles to become permeabilized before adding 99 µl of TE buffer and 1 µl of RiboGreen reagent to each well. Plates were shaken at room temperature for 5 min and fluorescence (excitation wavelength 485 nm, emission wavelength 528 nm) was measured using a plate reader (Biotek).

## 2.11. In vitro knockdown

RAW 264.7 cells (ATCC, TIB-71) (60% confluence) were treated with 0.2 µg/ml of siIRF8 or siNC5 entrapped in LNPs. After 24 h the cells were washed and activated with 2.5 ng/ml IFN $\gamma$  (Peprotech). 48 h after the transfection, cells were harvested and mRNA was isolated using EZ-RNA (Biological Industries), and cDNA was prepared using a cDNA synthesis kit (Quanta Biosciences). IRF8 mRNA levels were analyzed via RT-qPCR, normalized to mouse GAPDH as endogenous control. 72 h after transfection the medium was collected for cytokine analysis and the cells were taken to a dot blot assay.

## 2.12. Dot blot analysis

*In vivo*, *ex vivo* and *in vitro* samples were prepared using a solution of 150 mM NaCl, 50 mM Tris–HCl, 1 mM EDTA, 1% Triton X-100, 1% Na deoxycholic acid, protease inhibitor. Protein samples from 10 [5] cells were blotted onto a nitrocellulose membrane. After blocking in 5% low-fat milk in PBS buffer, the membrane was incubated with rabbit anti-mouse IRF8 antibodies (ThermoFisher) followed by HRP-conjugated goat anti-rabbit (Jackson ImmunoResearch), anti-mouse CD45

antibodies labeled with Alexa Flour 488 (Biolegend) and anti-Rat HRP (Jackson ImmunoResearch) as a control. ECL (Thermo Scientific Pierce) was used as a substrate solution. Signals were analyzed using Amersham Imager 600 (GE Healthcare Life Sciences) and PXi (Syngene) instruments.

## 2.13. Intracellular flow cytometry

72 h after transfection with LNPs (1 µg/ml siRNA), IRF8 protein levels were assessed via intracellular Flow cytometry. RAW 264.7 cells or primary mouse splenocytes were fixed and permeabilized using FoxP3/transcription factors fixation/permeabilization assay (eBioscience), stained with membrane antibodies and directly conjugated anti-IRF8 antibodies or isotype control. Fluorescence levels were analyzed using CytoFLEX instrument (Beckman Coulter).

## 2.14. IRF8 associated genetic pathways

In order to gain some insights on the anti-inflammatory mechanisms of IRF8 silencing, RAW 264.7 cells (ATCC, TIB-71) (60% confluence) were treated with 0.2 µg/ml of siIRF8 or siNC5 entrapped in LNPs. After 24 h the cells were activated with 2.5 ng/ml IFN $\gamma$  (Peprotech). 72 h after the transfection, cells were harvested and mRNA was isolated using EZ-RNA (Biological Industries), and cDNA was prepared using a cDNA synthesis kit (Quanta Biosciences). mRNA levels of Cybb, Spi1, CCL5, Slc11a1 and STAT1 were analyzed by RT-qPCR, normalized to mouse HPRT as endogenous control.

## 2.15. Animal experiments

All animal protocols were approved by Tel Aviv University Institutional Animal Care and Usage Committee and in accordance with current regulations and standards of the Israel Ministry of Health. All allocation and administered treatments. Mice were randomly divided in a blinded fashion in the beginning of each experiment.

## 2.16. Ex vivo experiments

siRNA loaded LNPs were incubated with fresh mouse serum for 30 min in 37 °C. Splenocytes from C57BL/6 mice, 2 × 10<sup>6</sup> cells/ml in RPMI supplemented with P/S/N, L-Glu, 1% sodium pyruvate, 1% NEAA, 0.1%  $\beta$ -mercaptoethanol (life-technologies), were incubated for 1 h with siIRF8 or siNC5 loaded LNPs (1 µg/ml). 1 h after transfection 10% FBS was added to the medium and 24 h later the cells were activated with 10 ng/ml LPS (Peprotech). IRF8 levels were analyzed 72 h after transfection by intracellular flow cytometry and dot blot western. Cytokines levels in the medium were analyzed 72 h after transfection using IL-6, TNF $\alpha$ , IL12p40 and IL1 $\beta$  ELISA kits (R&D Systems).

## 2.17. Confocal microscopy

Splenocytes from C57BL/6 mice were incubated for 30 min at 4 °C with LNPs encapsulating 15% NC5-cy5 siRNA, self-assembled with ASSET and  $\alpha$ Ly6C (bioXcell) or isotype control antibody (bioXcell). Cells were further stained with Hoechst 33342 (Sigma Aldrich) and Alexa Fluor 488  $\alpha$ Ly6C (Biolegend). Cells were washed, and images were analyzed using a Lecia SP8 confocal microscope (Lecia microsystems).

## 2.18. In vivo TsiLNPs binding

Cy5 labeled T-LNPs and I-LNPs were injected intravenously to C57BL/6 mice. 1 h after LNPs injection, splenocytes were isolated and stained with  $\alpha$ Ly6c (Biolegend) mAbs. Cy5 fluorescence levels in Ly6C<sup>+</sup> cells were analyzed using CytoFLEX instrument (Beckman Coulter).

### 2.19. *In vivo* IRF8 silencing

T-LNPs or I-LNPs, encapsulating siIRF8 or siNC5, were injected intravenously to 10-week-old C57BL/6 mice. 1 h after LNPs injection the mice were euthanized and leukocytes were harvested from the spleens. Splenic leukocytes were then sorted to Ly6C<sup>+</sup> and Ly6C<sup>-</sup> cells. The cells were cultured,  $2 \times 10^6$  cells/ml in RPMI supplemented with 10% FBS, P/S/N, L-Glu, 1% sodium pyruvate, 1% NEAA, 0.1%  $\beta$ -mercaptoethanol (life-technologies) and 10 ng/ml LPS (Peprotech), for 72 h and then lysed to evaluate IRF8 protein levels *via* western dot blot analysis.

### 2.20. IBD model

Colitis was induced in 10-week-old female C57BL/6 mice (Harlan laboratories) using dextran sodium sulphate (DSS). Mice were given 2% (wt/vol) DSS in the drinking water for 8 days. Suspensions (200  $\mu$ l in PBS) of TsiLNPs loaded with siRNAs against IRF8 or negative control siRNA NC5, and self-assembled with  $\alpha$ Ly6C or isotype control primary antibodies (BioXcell), were injected intravenously on days 3, 5 and 7 from the start on DSS treatment, at 1.5 mg/kg. Body weight was monitored every other day. On day 8 colitis severity was assessed by colonoscopy, using the Murine Endoscopic Index of Colitis (MEICS). All MEICS scoring was determined based on three impartial assessments. The length of the entire colon from cecum to anus was measured. Colons were homogenized using a lysis solution (150 mM NaCl, 50 mM Tris–HCl, 1 mM EDTA, 1% Triton x-100, 1% Na deoxycholic acid and protease inhibitor), to assess cytokines by IL-6, TNF $\alpha$ , IL12p40 and IL1 $\beta$  ELISA kits (R&D Systems). Splenocytes were isolated and stained with antibodies against CD45, CD11B, LY6C, CD3, CD4 and CD19 (Biolegend) for 30 min at 4 °C. Splenic leukocytes subsets were analyzed using flow cytometry (CytoFLEX instrument, Beckman Coulter).

### 2.21. Statistical analysis

All data are expressed as median  $\pm$  min to max or mean  $\pm$  SD. Statistical analysis for comparing two experimental groups was performed using two-sided Student's *t*-test. In experiments with multiple groups we used one-way ANOVA with Dunnett's multiple comparison post hoc test. Analyses were performed with Prism 5 (Graph pad Software). A value of  $p < 0.05$  was considered statistically significant. Differences are labeled \* for  $p \leq 0.05$ , \*\* for  $p \leq 0.01$ , \*\*\* for  $p \leq 0.001$  and \*\*\*\* for  $p \leq 0.0001$ . Sample size of each experiment was determined to be the minimal necessary for statistical significance by the common practice in the field. Similarity between variances of each statistically compared groups were verified by F test. Pre-established criteria for removal of animals from experiment were based on animal health, behavior and well-being as required by ethical guidelines; no animals were excluded from the experiments.

## 3. Results

### 3.1. Down regulating IRF8 *in vitro* via siRNA loaded LNPs

siRNA loaded LNPs were assembled using a microfluidic mixing of siRNA molecules and a lipid mixture (MC3, DSPC, Cholesterol, DMG-PEG, and DSPE-PEG at 50:10.5:38:1.4:0.1 mol ratio) under acidic conditions, using NanoAssemblr® system. The siRNA loaded LNPs were further characterized through DLS ( $57.63 \pm 3.2$  nm in diameter) with a  $\zeta$  potential of  $0.7 \pm 0.35$  mV, and visualized *via* TEM (Fig. 1, SI appendix, table S1). siRNA encapsulation efficiency was evaluated by RiboGreen assay ( $99 \pm 3.1$ ; SI appendix, table S1). The level of silencing IRF8 using siRNA loaded LNPs was assessed *in vitro* in Raw 264.7 cells. Raw 264.7 cells were incubated with 0.2  $\mu$ g / ml siRNA encapsulated in LNPs and were activated by 2.5 ng / mL IFN $\gamma$ . siIRF8-LNPs reduced IRF8 mRNA compared to negative control 5 siRNA (NC5si, IDT), by ~

90% (PV < 0.0001, n = 5, Fig. 1b). A notable reduction in IRF8 protein levels by IRF8 siRNA, compared to the NC5 siRNA control, was demonstrated using flow cytometry by an intracellular staining of IRF8 protein (Fig. 1c, SI appendix, Fig. S1a–b). IRF8 downregulation was accompanied with a noticeable decrease in TNF $\alpha$  pro-inflammatory cytokine as assayed by ELISA (n.s, SI appendix, Fig. S1c). To gain insights into the anti-inflammatory mechanism of IRF8 silencing in Raw 264.7 cells we analyzed the transcription levels of genes that were previously found to be regulated by IRF8 protein [23–27]. The mRNA levels of genes that were previously found to be associated with IRF8 protein were examined 72 h after LNPs transfection, by RT-PCR. These genes were chosen based on a comprehensive literature analysis and with the use of STRING database [28]. While the NC5 siRNA-loaded LNPs increased the transcription of *Cybb*, *Slc11a1*, and *Spi1* genes, IRF8 downregulation inhibited the transcription of these genes by 2, 2 and 1.6 folds, respectively (PV = 0.005, = 0.003, < 0.0001, respectively, n = 10, SI appendix, Fig. S2a–c). *CCL5* mRNA levels were significantly reduced by 1.5 folds with siNC5-LNPs treatment and 6-fold following IRF8 silencing (PV < 0.0001, n = 10, SI appendix, Fig. S2d). Furthermore, although upregulated by the NC5-siRNA loaded LNPs, a trend of *STAT1* downregulation by IRF8 silencing was seen (PV = 0.018, n = 10, SI appendix, Fig. S2e).

### 3.2. Anti-inflammatory effect by down regulating IRF8 *ex vivo*

To test whether IRF8 silencing has a therapeutic anti-inflammatory potential, we analyzed the effect of IRF8 downregulation on primary leukocytes *ex vivo*. Primary splenocytes, isolated from C57BL/6 mice were incubated with 1  $\mu$ g / mL siRNA loaded in LNPs, and were further activated by 10 ng / mL LPS. LPS was chosen as it demonstrates a wider spectrum of pro-inflammatory activation, which recapitulate better leukocytes activation in DSS treated mice. 72 h after transfection with LNPs the medium was collected for cytokine analysis and the cells were lysed for IRF8 protein levels analysis. siIRF8 but not siNC5 loaded LNPs mediated a notable reduction in IRF8 protein levels as demonstrated by dot blot assay, using splenocytes lysate (Fig. 1d). To assess the anti-inflammatory effect of IRF8 inhibition, we quantified pro-inflammatory cytokines in splenocytes conditioned media by ELISA (n = 4). Secreted TNF $\alpha$  levels were reduced by 23.5% with IRF8 silencing (PV = 0.0045), alongside a significant reduction in IL-6 medium concentration (PV = 0.0330, Fig. 1e–f). In addition, the concentration of the common subunit of IL-12 and IL-23, IL12p40, was decreased by 42.2% compared to NC5 control (Fig. 1g, PV < 0.0001).

### 3.3. Selective binding of antibody-targeted siRNA-loaded LNPs to Ly6C<sup>+</sup> leukocytes

Ly6C<sup>+</sup> leukocytes population was previously demonstrated to play an important pro-inflammatory role in IBD pathology [10,11]. Therefore, we aimed to selectively reprogram Ly6C<sup>+</sup> cells.  $\alpha$ Ly6C targeting antibody or isotype control were introduced to the LNPs using the ASSET platform to form targeted- (T-LNPs) and isotype control- (I-LNPs) (schematic illustration Fig. 2a, SI appendix, table S1). ASSET-LNPs were further characterized by TEM (Fig. 2b) and DLS and found to be  $64.95 \pm 2.4$  nm in diameter with a  $\zeta$  potential of  $0.6 \pm 0.22$  mV. siRNA encapsulation efficiency was evaluated by RiboGreen assay as  $98 \pm 1.7\%$  (SI appendix, table S1). The specificity of the T-LNPs to bind selectively Ly6C<sup>+</sup> cells was demonstrated previously [10,11] and further assessed *ex vivo* by confocal microscopy and *in vivo* by flow cytometry using Cy5 labeled LNPs (Fig. 2c–d, SI appendix, Fig. S3a–g). Cy5 T-LNPs, but not I-LNPs, bound selectively to Ly6C<sup>+</sup> cells. Furthermore, non-specific binding was not observed in Ly6C<sup>-</sup> cells (Fig. 2c–d, SI appendix, Fig. 3a–g). The flow cytometry analysis of TsiLNPs binding *in vivo* demonstrates a significant increase in Cy5 fluorescence signal of Ly6C<sup>+</sup> cells and can be appreciated by the movement of the Ly6C<sup>+</sup> population (Fig. S3e, g).

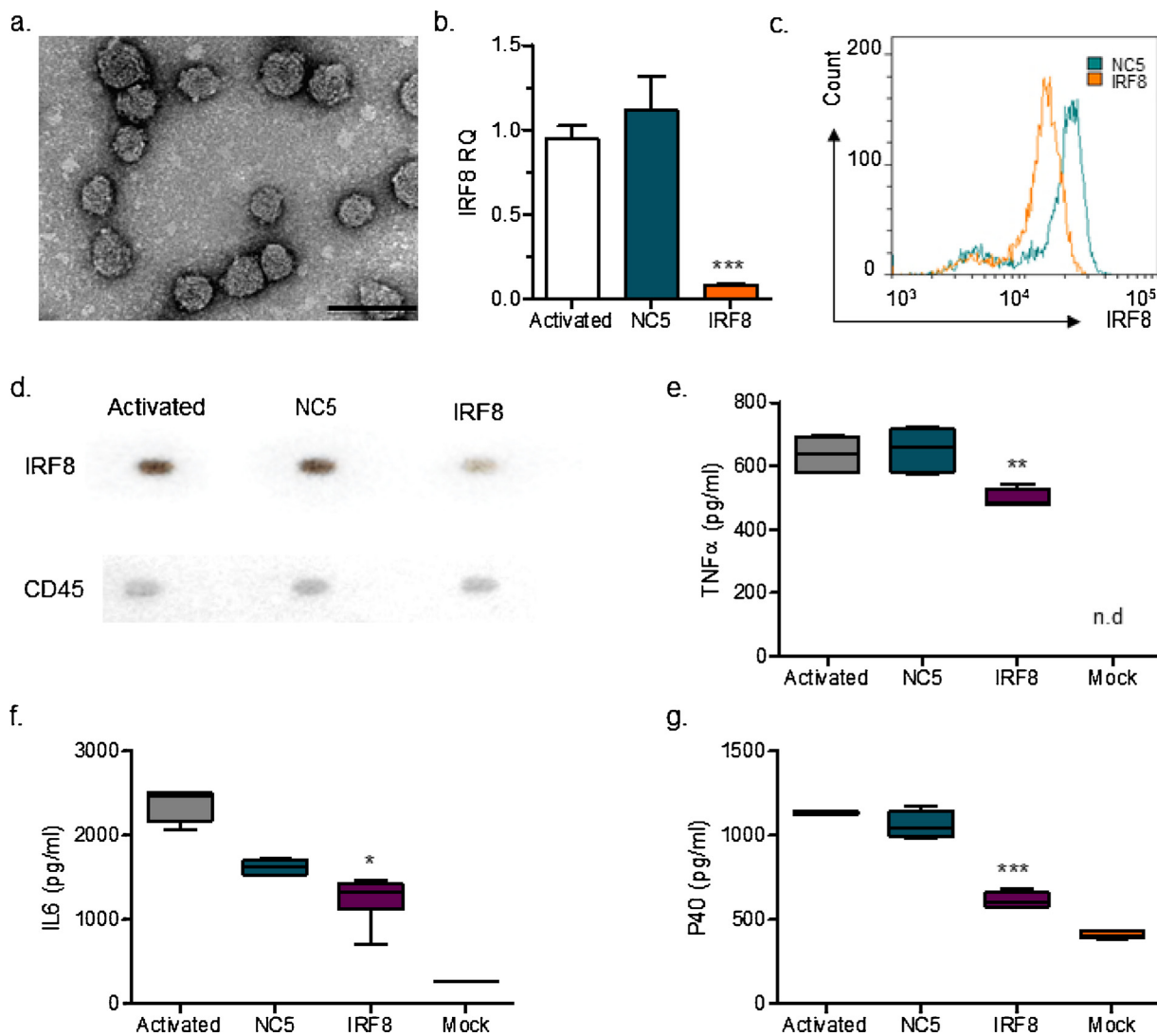


**Fig. 1.** Inhibition of IRF8 using siRNA loaded LNPs. (a). Representative transmission electron microscopy (TEM) images of siRNA loaded LNPs, scale bar 100 nm. (b) mRNA levels of IRF8 in RAW 264.7 cells as tested by quantitative polymerase chain reaction, RQ compared to activated RAW 264.7 cells. (c) representative intracellular flow cytometry evaluation IRF8 protein levels, following an incubation with siNC5 or siIRF8 loaded LNPs and activation using 2.5 ng/ml IFN $\gamma$ . Representative gating strategy of (c) displayed in supplementary Fig. 1 a–b. Data shown (b–c) demonstrate the comparison of RAW 264.7 cells treated with LNPs encapsulating siIRF8 (IRF8), LNPs encapsulating negative control siRNA (NC5), non-activated RAW 264.7 cells (Mock) and RAW 264.7 cells activated using IFN $\gamma$  (Activated). (d). Representative dot blot analysis of IRF8 and CD45 proteins levels follow a transfection of  $10^5$  murine splenocytes with NC5 or IRF8 siRNA loaded LNPs and activation with 10 ng/ml LPS. (e–g) Proinflammatory cytokines, TNF $\alpha$  (e), IL6 (f) and IL12p40 (g), secreted by LPS activated splenocytes, following a transfection with NC5 or IRF8 siRNA loaded LNPs. (d–g) data are shown for a culture of primary splenocytes, treated with LNPs encapsulating siIRF8 (IRF8) or negative control siRNA (NC5), non-activated (Mock) and LPS activated (Activated) primary splenocytes. Data are mean  $\pm$  s.d. (b) or interquartile range (IQR) with a median center line and min to max error bars (e–g). Statistical analysis was performed using one-way ANOVA with Dunnett’s multiple comparison, comparing all groups to IRF8 treatment; Significance symbols displayed represent the comparison of IRF8 and NC5 control. n = 5 (b) and n = 4 (e–g), \* denote  $p < 0.05$ , \*\* denote  $p < 0.01$ , \*\*\* denote  $p < 0.001$ . Data are representative of 3 independent experiments.

### 3.4. Selective reprogramming of Ly6C<sup>+</sup> cells

Following the anti-inflammatory effect observed *ex vivo*, and the establishment of a selective transfection of Ly6C<sup>+</sup> leukocytes, we chose to test the feasibility to reprogram Ly6C<sup>+</sup> cells through IRF8 inhibition. T-LNPs or I-LNPs, encapsulating siIRF8 or siNC5 as a control, were injected intravenously into C57BL/6 mice. Splenocytes were isolated 1 h after LNPs injection and sorted to Ly6C<sup>+</sup> and Ly6C<sup>-</sup> cells (SI appendix, Fig. S4a–c, gating strategy). The cells were cultured for 72 h and then lysed to evaluate IRF8 protein levels *via* western dot blot analysis which revealed a significant reduction in IRF8 levels, by T-LNPs encapsulating siIRF8, only in the Ly6C<sup>+</sup> cells (Fig. 3a–b), compared to CD45 protein levels. A minor reduction in IRF8 protein levels was noticed when using siNC5 T-LNPs and siIRF8 I-LNPs.

### 3.5. IRF8 is a potential anti-inflammatory target in DSS induced colitis mice

T-LNPs or I-LNPs, encapsulating siIRF8 or siNC5 as a control, were injected intravenously to Dextran Sodium Sulfate (DSS) induced mice (the timeline of the experiment is detailed in Fig. 3c). To assess the disease severity, the mice were weighed on a daily basis, and colon morphology was evaluated by colonoscopy on day 8 from the start of the DSS induction. After euthanization, colon-length was measured as a marker for inflammation and proteins were extracted from the colon using a lysis solution for further analysis. Although no difference in weight loss was observed (Fig. 3d), a significantly healthier colon morphology was observed in mice treated with T-LNPs encapsulated siIRF8, compared to the controls. Blinded assessment was performed *via* mouse colonoscopy evaluation and murine endoscopic index of colitis

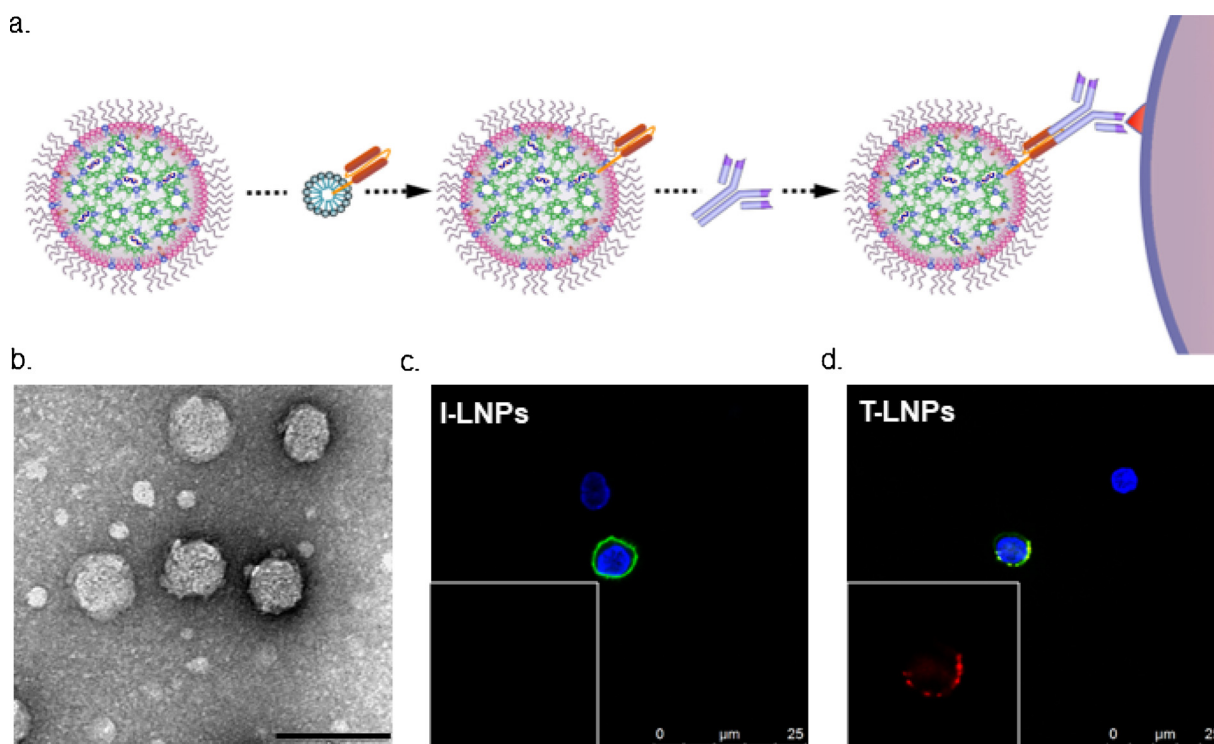


**Fig. 2.** Selective binding of siRNA loaded LNPs to Ly6C<sup>+</sup> expressing leukocytes. (a). Schematic illustration describing the self-assembly of ASSET into siRNA-loaded LNPs, binding of a primary antibody and a selective targeting of cell's receptor. (b). Representative transmission electron microscopy (TEM) images of siRNA loaded T-LNPs, scale bar: 100 nm. (c-d). Representative confocal microscopy images of murine splenocytes, incubated with cy5 (red) labeled ASSET LNPs conjugated to isotype control Ab (c) or anti Ly6C Ab (d). Splenocytes were also stained with Alexa Fluor 488 anti Ly6C Ab (green) and Hoechst nuclear staining (blue), scale bar: 25 μm. Box at the bottom left corner display only cy5 staining of the Ly6C<sup>+</sup> cells.

severity (MEICS) scoring. Mice treated with T-LNPs silencing IRF8 demonstrated ~20% improvement in colon length compared to the controls (PV < 0.0001, n = 5), and colonoscopy, with ~35% decrease in MEICS scoring, measuring five morphological parameters: the amount of colonic fibrin, colonic transparency, colonic blood vessels, colonic granularity, and feces' integrity (PV < 0.0001, n = 5, Fig. 3e–f). A profound improvement in colonic transparency as well as reduced amounts of colonic blood vessels and bleeding was demonstrated following a treatment with T-LNPs encapsulating siIRF8, compared to the controls (Fig. 3g).

Colonic pro-inflammatory cytokines were quantified as an indication for the severity of the intestinal inflammation (n = 5). Colonic TNFα levels were drastically reduced to baseline (PV < 0.0001, Fig. 4a). In addition, IRF8 silencing decreased the concentration of colonic IL6 cytokine and IL12p40 protein by ~60% and ~40%, respectively (PV < 0.0001, compared to T-NC5 control, Fig. 4b–c). A partial inhibition of colonic IL1β cytokine was demonstrated in all treatments, with a significant reduction by T-IRF8 treatment (PV = 0.02, Fig. 4d). Finally, the levels of Ly6C<sup>+</sup> inflammatory monocytes in the spleen were examined as an aspect of leukocytes recruitment from the bone marrow following a peripheral inflammation. Splenic population of CD11B<sup>+</sup> Ly6C<sup>+</sup> inflammatory monocytes was significantly lowered following the treatments with T-IRF8 LNPs (n = 4, PV < 0.05, Fig. 4e–f, SI appendix, Fig. S5a–c).

#### 4. Discussion

IRF8 transcription factor was previously demonstrated to have a central role in directing hematopoiesis towards the mononuclear phagocytic pathway as well as the differentiation of monocytes and several dendritic cells populations. Moreover, several studies implicated IRF8 in macrophages activation, supporting pro-inflammatory cytokines secretion and promoting Th1 and Th17 polarization in mice. Together

with valuable experimental data, human genetic analysis revealed a correlation between IRF8 genetic variations and an increase susceptibility to various inflammatory disorders, such as IBD. [15] Although several studies indicated IRF8 as a pro-inflammatory mediator in various diseases [17,18,20], a profound immunomodulation therapy through IRF8 inhibition was not demonstrated. Here we show, *via* targeted lipid nanoparticles approach, a therapeutic anti-inflammatory effect by IRF8 silencing in Ly6C<sup>+</sup> monocytes which were previously shown to play a critical role in IBD. IRF8 silencing *ex vivo* in leukocytes demonstrated promising anti-inflammatory properties, indicated by the decreased levels of inflammatory cytokines, which were previously shown to play a critical role in IBD. We have demonstrated a selective binding of TsiLNPs to Ly6C<sup>+</sup> cells *ex vivo* and *in vivo*. Due to reasonable technical reasons, the *ex vivo* binding experiment showed high binding capabilities that includes also a clustering of the receptors and the shielding of αLy6C labeled-mAbs binding, while the *in vivo* binding experiment showed a milder, and yet selective, TsiLNPs binding. This can be explained by the relative concentration of the LNPs, physiological conditions (such as temperature) and whole animal aspects such as LNPs' clearance. We established a selective delivery of siIRF8 loaded LNPs to Ly6C<sup>+</sup> cells and demonstrated how these LNPs mediated IRF8 downregulation in Ly6C<sup>+</sup> cells and an anti-inflammatory effect *in vivo*, in a murine colitis model. A slight decrease in IRF8 levels was detected in Ly6C<sup>+</sup> cells when using siIRF8 loaded I-LNPs and siNC5 loaded T-LNPs. This phenomenon can be explained by a minor unspecific uptake of I-LNPs by the phagocytic Ly6C<sup>+</sup> cells, and through the anti-inflammatory effect of αLy6C primary Abs conjugated to the LNPs, respectively. Yet, we have previously reported [10] that ASSET platform is shielding the Fc region of the Rat IgG2a mAbs from Fc receptors recognition. IRF8 silencing led to a significant decrease in the secretion of inflammatory cytokines, such as TNFα, IL6, IL12p40 and IL1β, both *ex vivo* and *in vivo*. While colonic IL1β was reduced in all treated groups to some extent, perhaps due to anti Ly6C Abs, which possess an anti-

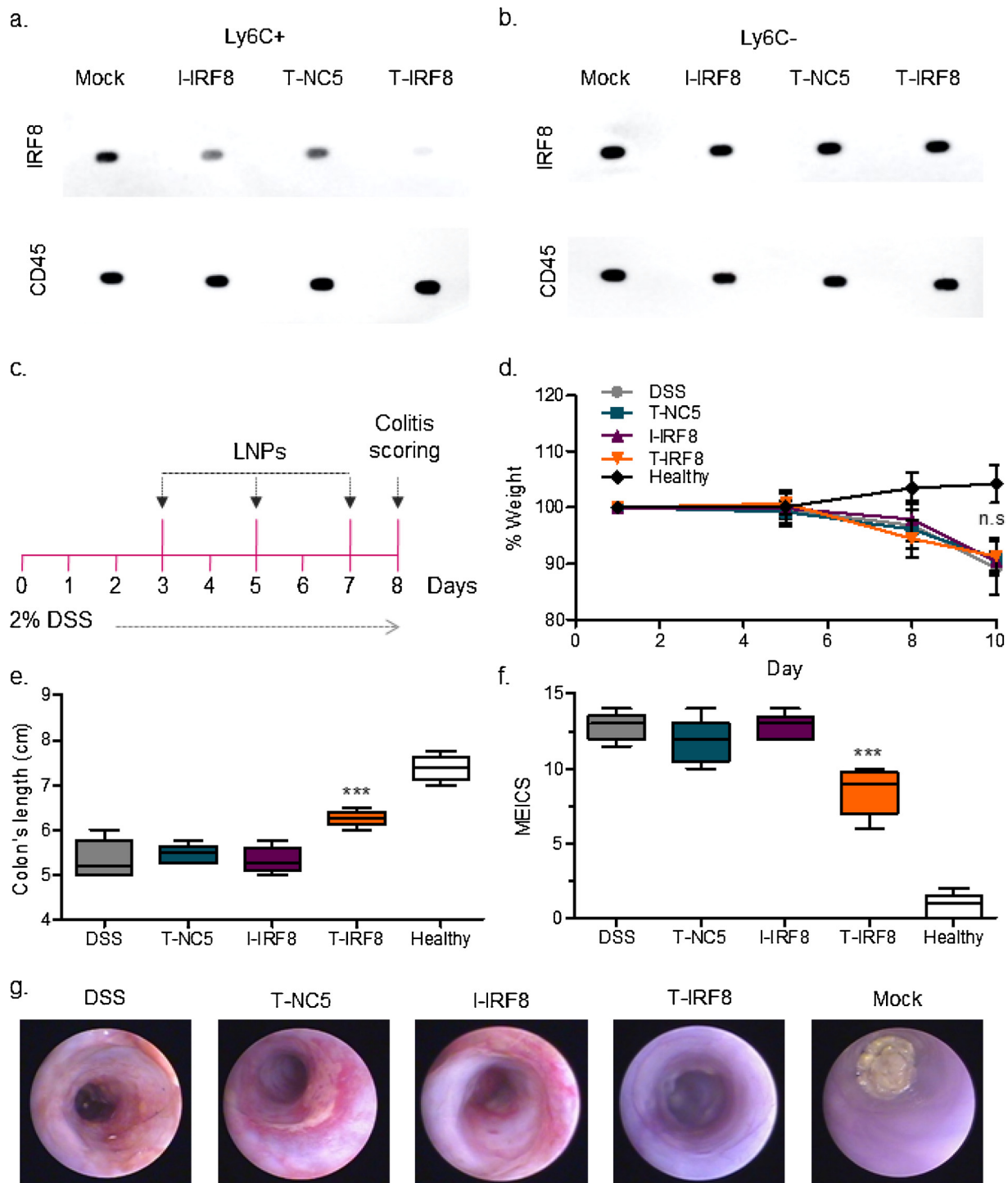


**Fig. 3.** Therapeutic potential of IRF8 inhibition in murine colitis model. (a–b) A selective IRF8 protein inhibition following intravenous injection of T-LNPs or I-LNPs, encapsulating siIRF8 or siNC5, is represented in a dot blot western analysis of  $10^6$  cells' lysate of Ly6C<sup>+</sup> (a) and Ly6C<sup>-</sup> (b) sorted splenocytes. CD45 levels were analyzed as control. Leukocytes were sorted from 4 mice in each group. Data in a–b are representative of 3 independent experiments. Gating strategy is represented in supplementary Fig. 4. (c). Experimental design. After initiating oral DSS, mice were injected intravenously with  $\alpha$ Ly6C or isotype control T-LNP encapsulating siIRF8 or siNC5 on days 3, 5, and 7 and were sacrificed on day 8. Body weight was measured daily (d) and colon length (e) was assessed on day 8. f. Colon's inflammation and morphology was assessed on day 8 by colonoscopy using Murine endoscopic index of colitis (MEICS). (g). Representative colonoscopy images. Data are Interquartile range (IQR) with a median center line and min to max error bars. Statistical analysis was performed using one-way ANOVA with Dunnett's multiple comparison, comparing all groups to T-IRF8 treatment; Significance symbols displayed represent the comparison of T-IRF8 and T-NC5 control.  $n = 5 / \text{group}$ ,  $n.s$   $p > 0.05$ , \*\*\* denote  $p < 0.001$ . Data are representative of 3 independent experiments.

inflammatory capability or the negligible unspecific uptake of the LNPs by phagocytic cells, a significant reduction was demonstrated with the siIRF8-loaded T-LNPs treatment. Moreover, the inhibition of IRF8 resulted in a decreased amount of circulating CD11b<sup>+</sup> Ly6C<sup>+</sup> cells.

Although no difference in weight loss was observed in the DSS colitis model, a significant improvement of colon's morphology was demonstrated. This phenomenon can be explained by the acute nature of the DSS model or perhaps by other pathways by which Ly6C<sup>+</sup> affect

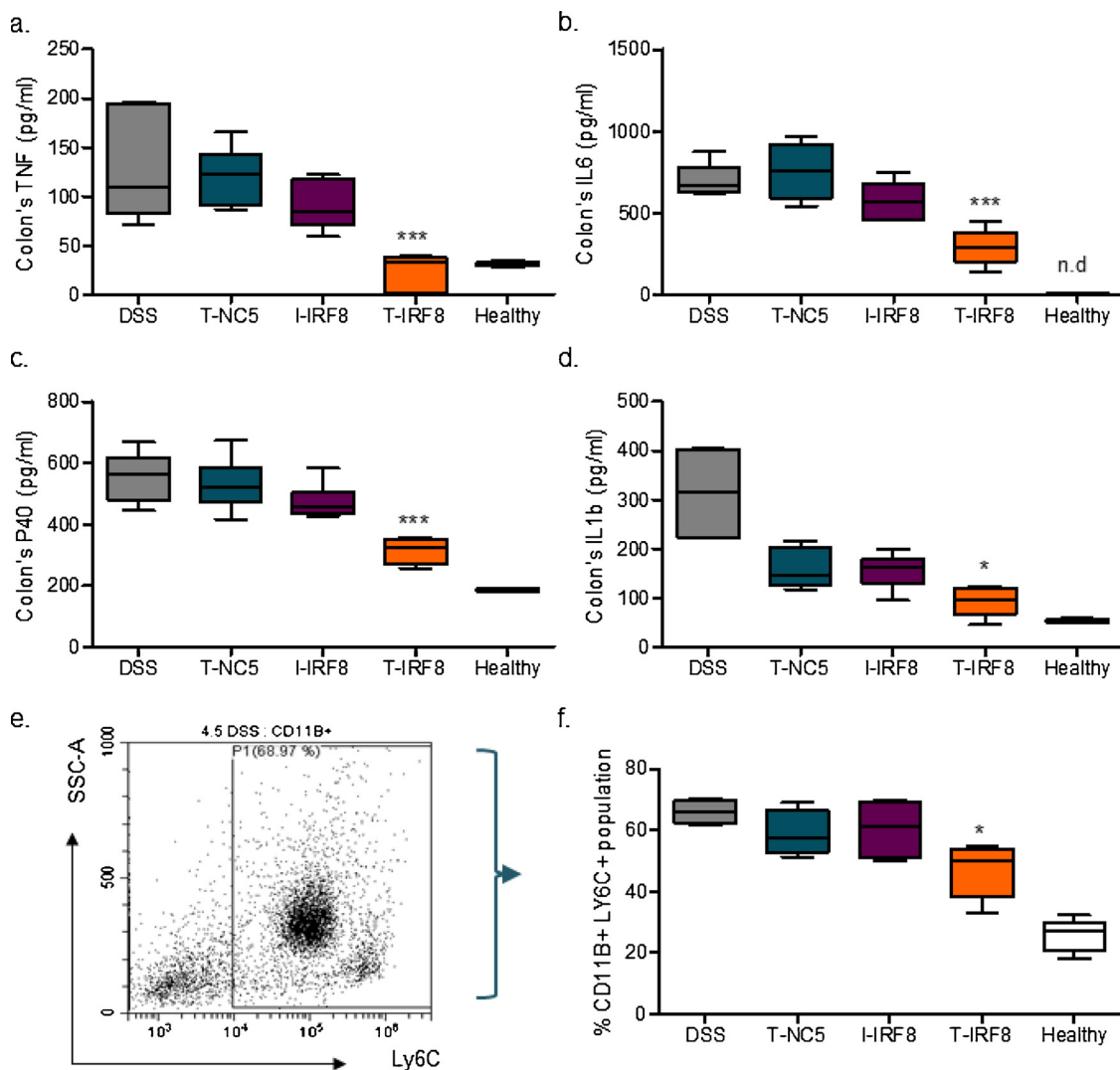


**Fig. 4.** Reduced pro-inflammatory phenotype by T-IRF8 treatment. Colonic levels of proinflammatory cytokines, TNF $\alpha$  (a), IL6 (b), IL-12/IL-23 p40 (c) and IL-1 $\beta$  (d), were assessed from a whole colon protein extract. e–f. Blood population of inflammatory CD11B<sup>+</sup> Ly6C<sup>+</sup> cells as assessed by flow cytometry. Representative flow cytometry graph for Ly6C<sup>+</sup> gating strategy (e). f. quantification of Ly6C<sup>+</sup> cells proportion in CD11B<sup>+</sup> population. Gating strategy for e–f are displayed in supplementary figure 5 a–c. Data are Interquartile range (IQR) with a median center line and min to max error bars. Statistical analysis was performed using one-way ANOVA with Dunnett's multiple comparison, comparing all groups to T-IRF8 treatment; Significance symbols displayed represent the comparison of T-IRF8 and T-NC5 control. n = 5 (a–d) and n = 4 (f), \* denote  $p < 0.05$ , \*\* denote  $p < 0.01$ , \*\*\* denote  $p < 0.001$ . Data are representative of 3 independent experiments.

metabolism and adipose tissues. Indications for siIRF8 anti-inflammatory mechanism were demonstrated in Raw 264.7 cells with the downregulation of the transcription of several known IRF8-related pathways, Cybb, Spi1, CCL5, Slc11a1 and STAT1. [23–27] While several of these inflammatory genes were upregulated due to the treatment with the LNPs, as can be expected in such artificial technique with the use of siRNA and ionizable cationic lipids [29–31], a clear downregulation of these pathways was demonstrated with the use of siIRF8. Moreover, it is likely that IRF8 downregulation induce changes in multiple inflammatory genes. This should be explored in a follow-up study.

While several studies identified IRF8 as a tumor suppressor gene, controlled downregulation of IRF8 in inflammatory leukocytes has a therapeutic potential for balancing the immune response and thus chronic inflammation [32,33]. For instance, IRF8 depletion in murine colonic epithelial cells was demonstrated to result in increased incidence of colon cancer [32]. However, our selective and transient T-LNPs approach for reprogramming Ly6C<sup>+</sup> inflammatory cells, via IRF8 silencing, has a potential to overcome such side effects and to mediate a profound anti-inflammatory effect.

In this study we have established a substantial transfection *ex vivo* of the notoriously hard to transfect leukocytes. This technique can serve as a valuable research tool for a wide range of applications. We further demonstrated how our versatile gene manipulation platform, ASSET-based T-LNPs, can be utilized to identify new therapeutic targets, such as IRF8. Altogether, we propose that siIRF8 loaded T-LNPs, targeting inflammatory Ly6C<sup>+</sup> cells, can serve as a new immunomodulatory modality for treating IBD and other inflammatory disorders. Furthermore, we have demonstrated the research capabilities of our targeting platform, serving not only as a powerful therapeutic technology but also as a research tool, capable of characterizing new targets for potential therapy.

#### Authors contribution

N.V. and D.P. conceived the study. N.V., M.G. and S.R. performed the research, N.V., Y.D., E.E., M.B., I.B. and D.P. analyzed the data. N.V., Y.D., D.R. and D.P. wrote the manuscript.

## Data and material availability

All relevant data are available from the authors upon reasonable request.

## Declaration of competing interest

D.P. declare financial interest in Quiet Therapeutics and ART Biosciences. The rest of the authors declare no other conflict of interests.

## Acknowledgments

N.V. thanks the Marian Gertner Institute of Medical Nanosystems, the Dan David Fellowship Award, the Bruce and Ruth Rappaport Foundation and Iafa Keidar Prize for all their support.

This work was supported in part by grants from The Dotan Center for Hemato-Oncology at Tel Aviv University; and by the ERC grant LeukoTheranostics (# 647410) awarded to DP.

## Appendix A. Supplementary data

Supplementary material related to this article can be found, in the online version, at doi:<https://doi.org/10.1016/j.jconrel.2019.10.001>.

## References

- [1] Y.A. Yap, E. Marino, An insight into the intestinal web of mucosal immunity, microbiota, and diet in inflammation, *Front. Immunol.* 9 (2617) (2018).
- [2] J. Pazmandi, A. Kalinichenko, R.C. Ardy, K. Boztug, Early-onset inflammatory bowel disease as a model disease to identify key regulators of immune homeostasis mechanisms, *Immunol. Rev.* 287 (2019) 162–185.
- [3] R. Weisshof, K. El Jurdi, N. Zmeter, D.T. Rubin, Emerging therapies for inflammatory bowel disease, *Adv. Ther.* 35 (2018) 1746–1762.
- [4] C.C. Bain, A. Schridde, Origin, Differentiation, and Function of Intestinal Macrophages, *Front. Immunol.* 9 (2018) 2733.
- [5] A.A. Kuhl, U. Erben, L.I. Kredel, B. Siegmund, Diversity of intestinal macrophages in inflammatory bowel diseases, *Front. Immunol.* 6 (2015) 613.
- [6] M.K. Magnusson, et al., Macrophage and dendritic cell subsets in IBD: ALDH+ cells are reduced in colon tissue of patients with ulcerative colitis regardless of inflammation, *Mucosal Immunol.* 9 (2016) 171–182.
- [7] A. Schippers, et al., beta7-Integrin exacerbates experimental DSS-induced colitis in mice by directing inflammatory monocytes into the colon, *Mucosal Immunol.* 9 (2016) 527–538.
- [8] A. Waddell, et al., Colonic eosinophilic inflammation in experimental colitis is mediated by Ly6C(high) CCR2(+) inflammatory monocyte/macrophage-derived CCL11, *J. Immunol.* (Baltimore, Md. : 1950) 186 (2011) 5993–6003.
- [9] G.R. Jones, et al., Dynamics of Colon monocyte and macrophage activation during colitis, *Front. Immunol.* 9 (2018) 2764.
- [10] R. Kedmi, et al., A modular platform for targeted RNAi therapeutics, *Nat. Nanotechnol.* 13 (2018) 214–219.
- [11] N. Veiga, et al., Cell specific delivery of modified mRNA expressing therapeutic proteins to leukocytes, *Nat. Commun.* 9 (2018) 4493.
- [12] T.M. Nowacki, et al., The 5A apolipoprotein A-I (apoA-I) mimetic peptide ameliorates experimental colitis by regulating monocyte infiltration, *Br. J. Pharmacol.* 173 (2016) 2780–2792.
- [13] D. Sichien, et al., IRF8 transcription factor controls survival and function of terminally differentiated conventional and plasmacytoid dendritic cells, *Respectively, Immunity* 45 (2016) 626–640.
- [14] N. Hagemeyer, et al., Transcriptome-based profiling of yolk sac-derived macrophages reveals a role for Irf8 in macrophage maturation, *EMBO J.* 35 (2016) 1730–1744.
- [15] P.S. Ramos, A.M. Shedlock, C.D. Langefeld, Genetics of autoimmune diseases: insights from population genetics.
- [16] Y. Guo, et al., Inhibition of IRF8 negatively regulates macrophage function and impairs cutaneous wound healing, *Inflammation* 40 (2017) 68–78.
- [17] Y. Jia, et al., IRF8 is the target of SIRT1 for the inflammation response in macrophages, *Innate Immun.* 23 (2017) 188–195.
- [18] H. Xu, et al., Notch-RBP-J signaling regulates the transcription factor IRF8 to promote inflammatory macrophage polarization, *Nat. Immunol.* 13 (2012) 642–650.
- [19] D. Kurotaki, et al., Essential role of the IRF8-KLF4 transcription factor cascade in murine monocyte differentiation, *Blood* 121 (2013) 1839–1849.
- [20] Y. Yoshida, et al., The transcription factor IRF8 activates integrin-mediated TGF-beta signaling and promotes neuroinflammation, *Immunity* 40 (2014) 187–198.
- [21] S. Ramishetti, et al., Systemic gene silencing in primary T lymphocytes using targeted lipid nanoparticles, *ACS Nano* 9 (2015) 6706–6716.
- [22] S. Weinstein, et al., Harnessing RNAi-based nanomedicines for therapeutic gene silencing in B-cell malignancies, *Proc. Natl. Acad. Sci. U. S. A.* 113 (2016) E16–22.
- [23] M.F.M. Cellier, Developmental control of NRAMP1 (SLC11A1) expression in professional phagocytes, *Biology* 6 (2017).
- [24] G. Chen, C.S. Tan, B.K. Teh, J. Lu, Molecular mechanisms for synchronized transcription of three complement C1q subunit genes in dendritic cells and macrophages, *J. Biol. Chem.* 286 (2011) 34941–34950.
- [25] S. Chmielewski, et al., STAT1-dependent signal integration between IFNgamma and TLR4 in vascular cells reflect pro-atherogenic responses in human atherosclerosis, *PLoS One* 9 (2014) e113318.
- [26] D. Langlais, L.B. Barreiro, P. Gros, The macrophage IRF8/IRF1 regulome is required for protection against infections and is associated with chronic inflammation, *J. Exp. Med.* 213 (2016) 585–603.
- [27] W.I. Lee, et al., Immune defects in active mycobacterial diseases in patients with primary immunodeficiency diseases (PIDs), *J. Formos. Med. Assoc.* 110 (2011) 750–758.
- [28] D. Szklarczyk, et al., STRING v11: protein-protein association networks with increased coverage, supporting functional discovery in genome-wide experimental datasets, *Nucleic Acids Res.* 47 (2019) D607–d613.
- [29] H.Y. Xue, S. Liu, H.L. Wong, Nanotoxicity: a key obstacle to clinical translation of siRNA-based nanomedicine, *Nanomedicine* (London, England) 9 (2014) 295–312.
- [30] D. Peer, Immunotoxicity derived from manipulating leukocytes with lipid-based nanoparticles, *Adv. Drug Deliv. Rev.* 64 (2012) 1738–1748.
- [31] R. Kedmi, N. Ben-Arie, D. Peer, The systemic toxicity of positively charged lipid nanoparticles and the role of Toll-like receptor 4 in immune activation, *Biomaterials* 31 (2010) 6867–6875.
- [32] M.L. Ibrahim, et al., Myeloid-derived suppressor cells produce IL-10 to elicit DNMT3b-Dependent IRF8 silencing to promote colitis-associated Colon tumorigenesis, *Cell Rep.* 25 (2018) 3036–3046 e3036.
- [33] C. Gaillard, et al., Identification of IRF8 as a potent tumor suppressor in murine acute promyelocytic leukemia, *Blood Adv.* 2 (2018) 2462–2466.